

Multifractality can be a universal signature of phase transitions

Zhi Chen¹ and Xiao Xu¹

¹*Department of Modern physics, University of Science and Technology of China, Hefei, Anhui 230026, China*

Macroscopic systems often display phase transitions where certain physical quantities are singular or self-similar at different (spatial) scales. Such properties of systems are currently characterized by some order parameters and a few critical exponents. Nevertheless, recent studies show that the multifractality, where a large number of exponents are needed to quantify systems, appears in many complex systems displaying self-similarity. Here we propose a general approach and show that the appearance of the multifractality of an order parameter related quantity is the signature of a physical system transiting from one phase to another. The distribution of this quantity obtained within suitable (time) scales satisfies a q -Gaussian distribution plus a possible Cauchy distributed background. At the critical point the q -Gaussian shifts between Gaussian type with narrow tails and Lévy type with fat tails. Our results suggest that the Tsallis q -statistics, besides the conventional Boltzmann-Gibbs statistics, may play an important role during phase transitions.

Phase transitions are ubiquitous in physical systems. A first general theory of phase transitions is the mean field theory, from which in the vicinity of the critical point the free energy can be expanded in a power series of a universal quantity called “order parameter” [1]. This quantity fluctuates around zero in a “disordered” phase above the critical point, and is non-zero in an “ordered” phase below the critical point representing the broken symmetry. Unfortunately the predictions from this theory are often not correct when comparing with experiments. To remedy this, much progress has been made in the theory of phase transitions during last fifty years with the landmark of the discovery of some universal scaling laws and the introduction of the renormalization group method [2–4]. With them the seemingly complex phase transitions in a variety of systems can be quantified by a few critical exponents which represent the self-similar characteristics of systems during transitions. Recently, such ideas of statistical physics have been applied to many complex systems in various fields and have extensively expanded the understanding to these systems [5]. Yet, these studies indicate that in many cases a few scaling exponents representing the self-similarity fail to quantify certain property of systems. Instead, one needs a large number (spectrum) of scaling exponents to clarify the characteristic of systems which represents a higher level of complexity. Examples include the processes of diffusion-limited aggregation (DLA) [6], turbulence and chaos [7, 8], Human heartbeat dynamics [9], climate change [10] and many financial quantities such as stock prices [5]. This characteristic has been called “multifractality”. A natural question is thus whether such behaviour can be seen in phase transitions. During last two decades people have verified the multifractality of certain quantities on some specific transitions such as random field transitions [11] and Anderson transitions at the critical point [12–15]. However, a general interpretation is still absent on how the multifractality appears with phase transitions. Especially, is the multifractality a universal property of phase transitions as those scaling laws? To address these questions, we argue that one should investigate the property of systems which appears universally in phase transitions. The only ideal quantity to our knowledge is the order parameter.

Another important progress recently in statistical physics is non-extensive Tsallis q -statistics [16, 17], which is a gen-

eralization of the conventional Boltzmann-Gibbs statistics. Specifically, when the effective number of degrees of freedom is small, one obtains the Tsallis q -statistics following the same arguments to obtain the Boltzmann-Gibbs statistics [18, 19]. In this frame some variables such as the entropy and the energy, may be non-extensive when systems have long-range correlations [20]. It is well-known that the correlation length is infinite at the critical point of a continuous transition. Thus, systems near the critical point are ideal candidates to observe such non-extensive behaviour. Just as the limit distribution of the sum of independent and identically distributed variables is Gaussian or Lévy-stable distribution, in q -statistics where the long-range correlation is present we observe a q -Gaussian distribution [21]. The distributions related to Tsallis q -statistics have been observed in many experiments, such as cold atoms in dissipative optical lattices [22], superdiffusion [23], solar plasma dynamics [24], spin glass relaxation [25], tissue radiation response [26], and financial signals [5, 27].

Here we show that, at temperatures near the critical point the distribution of an order parameter related quantity satisfies a q -Gaussian distribution plus a possible Cauchy background. At the critical point, the distribution shifts between the Lévy regime and the Gaussian regime [28, 29], triggering the multifractal behaviour and signalling the phase transition.

Distribution and the measuring quantity

The q -Gaussian distribution of interest is a symmetric distribution and has the following form:

$$f_q(D) = P_0 \cdot [1 + (q - 1)(D - D_0)^2 / 2\sigma^2]^{-\frac{1}{q-1}}, \quad (1)$$

where σ is a scale parameter related to the variance of the distribution, D_0 indicates the peak position, and P_0 is a normalization parameter. Letting $q \rightarrow 1$ one recovers the Gaussian distribution. When $q \in [1, 5/3)$, the distribution is in the Gaussian regime. The signal is monofractal and can be described by a single exponent. The distribution falls into the Lévy regime with infinite variance when $q \in (5/3, 3)$, and the critical value is $q_c = 5/3$ [17]. In this regime $f_q(D)$ decays asymptotically as that of a Lévy-stable distribution. Specifically the Cauchy distribution corresponds to $f_2(D) = \gamma / \{\pi[(D - D_0)^2 + \gamma^2]\}$ where $\gamma = \sqrt{2}\sigma$ is a scale parameter. It has been shown that the signal with the

q -Gaussian distribution in the Lévy regime is multifractal [28–30]. The multifractal behaviour is manifested by two attractors at $(\alpha, f(\alpha)) = (0, 0)$ and $((q-1)/(3-q), 1)$, where α is the singularity strength and $f(\alpha)$ is the singularity spectrum [29]. Further, the multifractality may survive even when the time correlation is destroyed by shuffling the data [29].

We hypothesize a universal measuring quantity which possibly satisfies a q -Gaussian distribution as follows. It contains only the order parameter and does not depend on details of a specific system, thus should be a dimensionless quantity. We further utilize the “universal” self-similar property of certain physical quantities of the system near the phase transition. This implies that such property does not change when the measuring scale alters. Combining these ideas we construct the desired quantity as the ratio of two order parameters measured at different spatial scales. Its distribution $P(D) = P(m_1/m_b)$ where m_1 and m_b are order parameters m measured at scale 1 and scale $b > 1$, respectively.

When far away from the critical point the distribution of an order parameter should be Gaussian at different spatial scales. Its mean is zero in a disordered phase and non-zero in an ordered phase. Thus in the disordered phase $P(D)$ satisfies a Cauchy distribution. In the ordered phase, we mark the mean and the fluctuations of the order parameter at the scale “1” (scale “ b ”) as x_0 and $\delta_x(t)$ [y_0 and $\delta_y(t)$], respectively. For sufficiently large systems $x_0 \gg \delta_x(t)$ and $y_0 \gg \delta_y(t)$. Thus the ratio D is:

$$\frac{x_0 + \delta_x(t)}{y_0 + \delta_y(t)} = \frac{x_0}{y_0} + \frac{y_0\delta_x(t) - x_0\delta_y(t)}{y_0^2} + \mathcal{O}\left(\frac{x_0\delta_y(t)^2 - y_0\delta_x(t)\delta_y(t)}{y_0^3}\right). \quad (2)$$

From equation (2) we find that in the ordered phase $P(D)$ to the first order of δ is a Gaussian. Therefore, in two extreme cases, $P(D)$ satisfies a q -Gaussian distribution. We next investigate how $P(D)$ behaves when the system is near the critical point from some tunable examples.

Example tunable models

We now focus on some tunable examples of finite size spin systems to verify our hypothesis. For all models we obtain the data through Monte Carlo simulations and apply periodic boundary conditions to systems of different sizes. When the size $L \rightarrow \infty$ one obtains the property of a macroscopic system. The system at the scale “1” is the original spin system, and the block spin system at the scale “ b ” is constructed using the standard coarse-graining operation in statistical physics [2–4] (see the Appendix A).

We investigate two well-known models: (1) The 2-dimensional nearest-neighbour Ising model with the Hamiltonian $H = -J \sum_{\langle ij \rangle} s_i s_j$, where $\langle ij \rangle$ represents nearest neighbours, ferromagnetic parameter $J = 1$ and the spin $s_i = \pm 1$. This model has a second order phase transition at $T_c = 2J/[\ln(1 + \sqrt{2})]$. The temperature is in units of $1/k_B$ where k_B is the Boltzmann constant. Its order parameter is the magnetization (per site) and we obtain the time series using

the Wolff algorithm [31]. The ratio $D(t) = m(1, t)/m(b, t)$ where $m(b, t)$ and $m(1, t)$ are order parameters measured at the same Monte Carlo step (MCS) “ t ”. (2) The 3-dimensional nearest-neighbour Ising glass model which has a second order phase transition with very slow dynamics near the critical point [32, 33]. Its $T_c = 0.95$ and the Hamiltonian $H = -\sum_{\langle ij \rangle} J_{ij} s_i s_j$ where we set J_{ij} satisfying a Gaussian distribution with zero mean and unit variance, and the spin $s_i = \pm 1$. Each configuration of J_{ij} is one sample. At each temperature after the equilibrium we simulate 150 samples with at least two million MCS per sample. The order parameter is the spin overlap $m = (\sum_i s_i^{(1)} s_i^{(2)})/N$ where $\{s_i^{(2)}\}$ is a replica of $\{s_i^{(1)}\}$, N is the number of spins. The order parameter time series are obtained using the Metropolis algorithm [34].

We also provide another model as a representing scenario for general cases of phase transitions. The example is the 2-dimensional nearest-neighbour n -state Potts model where n is a positive integer and each spin takes values $0, 1, \dots, n-1$. This model has a second order transition for $n \leq 4$ and a first order transition for $n > 4$ [35]. Specifically, when $n = 2$ it returns to the Ising model. Its $T_c = J/[\ln(1 + \sqrt{n})]$, the Hamiltonian $H = -J \sum_{\langle ij \rangle} \delta_{s_i, s_j}$ and we set $J = 1$. The order parameter is $m_{i, \alpha} = (n \times \langle \delta(s_i, \alpha) \rangle_T - 1)/(n-1)$ where i is the index of a spin, α is the value that the spin can take and $\langle \dots \rangle_T$ indicates a thermal average [36]. The order parameter series are obtained using the Metropolis algorithm [34]. Due to the spin symmetry, we obtain $P(D)$ utilizing all $D_{ij}(t) = m_{i, \alpha}(1, t)/m_{j, \alpha}(b, t)$ where j is the index of the block spin, i is the index of any original spin within the block spin j . We have fixed the value of α in the calculation.

In the simulations we set the rescaling factor $b = 4$ for the Ising model and the Potts model, and $b = 2$ for the glass model.

$P(D)$ near the critical point

Results of $P(D)$ for the Ising model near the critical point are shown in Fig. 1a and in the Appendix B. When approaching the critical point from the ordered phase ($T < T_c$), a Gaussian fit to $P(D)$ gradually does not work well, and it is worse when $T > T_c$. In these situations the testing Gaussian fit underestimates $P(D)$ at the peak, overestimates $P(D)$ on two shoulders, and diminishes faster than the exponential decay compared to the decay of $P(D)$ which contains power-law tails. Instead, a q -Gaussian fit coincides very well with the central part of $P(D)$ at all temperatures. We observe an increasing value of the parameter q with increasing temperature. At $q = 5/3$ the q -Gaussian enters Lévy regime with infinite variance, and we take this point as our critical temperature $T_{c, q}^L$ for the finite system with the size L . Thus from this specific example, we find that near the critical point the order parameter ratio D is our desired quantity.

When the ratio D is very far away from the peak D_0 , we find that $P(D)$ separates from such q -Gaussian fit. At all temperatures we observe that fat tails of $P(D)$ decay as D^{-2} , suggesting possible “universal” origin. Since in the disordered phase $P(D)$ follows a Cauchy distribution, we fit these

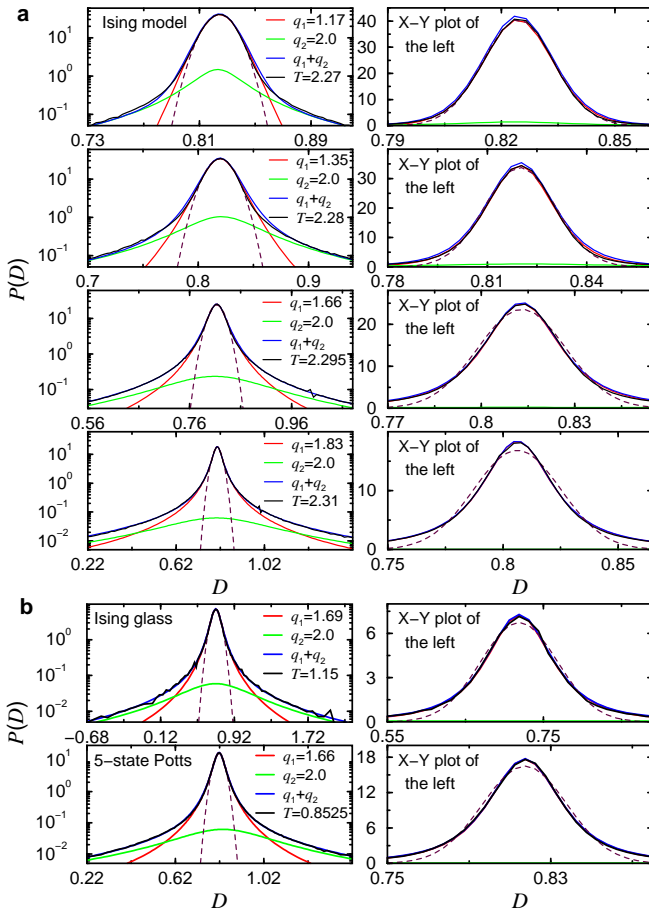


FIG. 1: Distributions of the order parameter ratio $P(D)$. **a**, At different temperatures for the 2-dimensional Ising model with the size $L = 124$. **b**, At the critical temperature $T_{c,q}^L$ for the 3-dimensional Ising glass model with the size $L = 12$, and the 2-dimensional 5-state Potts model with the size $L = 48$ and the thermal averaging interval $N_{tw} = 80,000$. The lengths of the order parameter ratio for three models are 8-16 million, 150 samples each with 2 million points, and 5.8 million, respectively. At all temperatures the central part of $P(D)$ can be well fitted by a q -Gaussian distribution, and the fat tails can be well fitted by a Cauchy distribution. Summation of the two provides a good fit at all ranges and at all temperatures. A Gaussian fit (dashed line) to the central part does not work when T approaches $T_{c,q}^L$ and when $T > T_{c,q}^L$. More details of the tails for the same distributions see the Appendix B.

fat tails with this distribution and take them as background. The Cauchy fits work well even when $P(D) \sim 10^{-5}$ (see the Appendix B). As shown in Fig. 1a, the summation of a q -Gaussian distribution and a suitable Cauchy background at each temperature of interest provides good fit to $P(D)$ in all ranges of D , i.e., $P(D) = (1-p)f_q(D) + pf_2(D)$ where $f_2(D)$ is due to the Cauchy tails and p is the probability of the Cauchy contribution. This implies that the central part and tails part of $P(D)$ may be independent. By reversing our procedure we can deduce the origin of the Cauchy part (see the Appendix C). We find that the distribution of $m(1, t)$ or $m(b, t)$ which contributes to the Cauchy part outside the cross points with the central part of $P(D)$ achieves a local maxi-

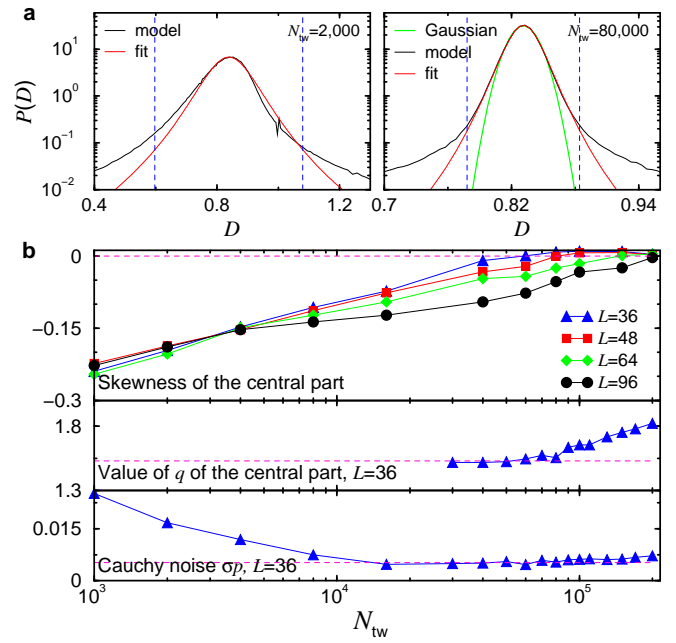


FIG. 2: Characteristics of $P(D)$ for the 5-state Potts model measured with different thermal averaging interval N_{tw} . **a**, Asymmetric and symmetric distributions with different N_{tw} for the 5-state Potts model at $T = 0.8495$ ($q = 1.3$). The system size is $L = 48$ and the red lines are q -Gaussian fits. **b**, Dependence of different parameters on the value of N_{tw} where we fix the temperature $T = 0.8515$.

um and is symmetric about zero, indicating a disorder-like behaviour. It decays with approximately exponential tails for large values of m and decays faster for the larger system.

Similar considerations can be done on both the Ising glass model and the Potts model. We find that the ratio distributions of them both share the similar behaviour with that of the Ising model. The Gaussian distribution could not fit the central part of $P(D)$ at temperatures near the critical temperature $T_{c,q}^L$. This is true even for the 5-state Potts model which has a first order phase transition. In Fig. 1b we show the fits at $T_{c,q}^L$ for both models. When approaching $T_{c,q}^L$ we observe Cauchy distributed fat tails where the ratio D is far away from the peak D_0 . Further, combining a q -Gaussian distribution and a suitable Cauchy background provides a good fit to $P(D)$ at all ranges of D . Nevertheless, for the Potts model, one has to choose a suitable thermal averaging interval N_{tw} (in units of MCS) for the order parameter. For the 5-state Potts model with the size $L = 48$ we take $N_{tw} = 80,000$ at all temperatures.

General scenario

As shown in Fig. 2a, $P(D)$ taken with randomly chosen N_{tw} , e.g., $N_{tw} = 2,000$ for the 5-state Potts system with the size $L = 48$, may be asymmetric thus would not follow a q -Gaussian distribution. With the Potts model as an example, here we propose an approach which can be applied to general physical systems.

First, from the construction of our measuring quantity we hypothesize that the possible “universal” q -Gaussian distribu-

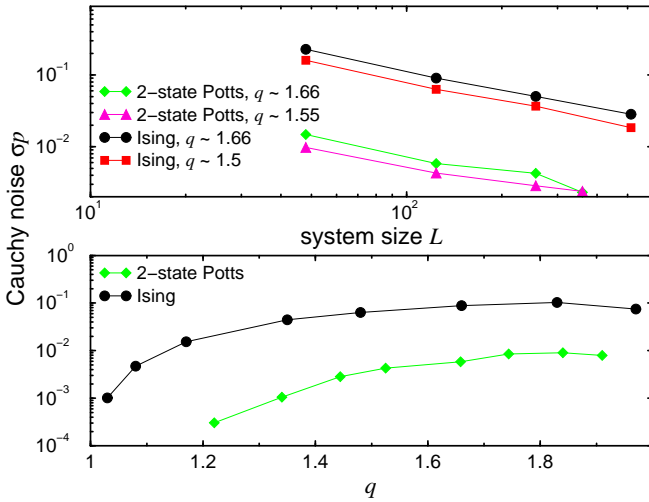


FIG. 3: Characteristics of the Cauchy noise strength in $P(D)$ within suitable range of N_{tw} . The Cauchy noise strength is proportional to the σ_p of the noise where D is far away from the peak D_0 and is invariant within suitable range of N_{tw} . Here we show the dependence of the σ_p of the Cauchy noise on the system size L for fixed q , and its dependence on the value of q for fixed $L = 124$ and $N_{tw} = 15,000$.

tion is relevant to the self-similarity of certain physical quantities near the transition. To verify this, we investigate the self-similarity of the distribution $P(m)$ of the order parameter m at different spatial scales and find that it is broken for small values of N_{tw} (see the Appendix A). Correspondingly we obtain asymmetric $P(D)$. The self-similarity of $P(m)$ becomes better for larger values of N_{tw} . When $N_{tw} = 150,000$ for the 5-state Potts model with the size $L = 96$ the distributions $P(m)$ at two scales are almost identical after the rescaling. Correspondingly $P(D)$ becomes symmetric.

We thus next quantify how $P(D)$ responds when the value of N_{tw} alters. To do this, we calculate the skewness of the central part of $P(D)$. As examples shown in Fig. 2a, the considered region is within two dashed lines. We fix the temperature and study how the skewness changes with different values of N_{tw} (see the Appendix D for relevant details). For different sizes of systems we find that the skewness is closer to zero for larger value of N_{tw} . For sufficiently large $N_{tw} \geq N_{tw}^{\min}$ the skewness stays at around zero, while $P(D)$ is symmetric and its central part follows a q -Gaussian distribution. The value of N_{tw}^{\min} seems larger for larger size of systems and it is comparable with the characteristic time scale of the order parameter m (see the Appendix E). Specifically, for the 2-state Potts model N_{tw}^{\min} is around the number of spins (see the Appendix D), thus the results of the 2-state Potts model is consistent with that of the Ising model. Starting from N_{tw}^{\min} , some specific short-range properties of the Potts model are lost and the q value from a q -Gaussian fit to $P(D)$ keeps constant in a broad range of N_{tw} (see Fig. 2b). Thus we consider the value of q obtained with N_{tw} chosen in such range as the suitable value of q . When N_{tw} further increases, however the value of q will increase. In this situation the order parameter itself is gradually not a good quantity to quantify the system. The above are remarks how we should choose the order parameters.

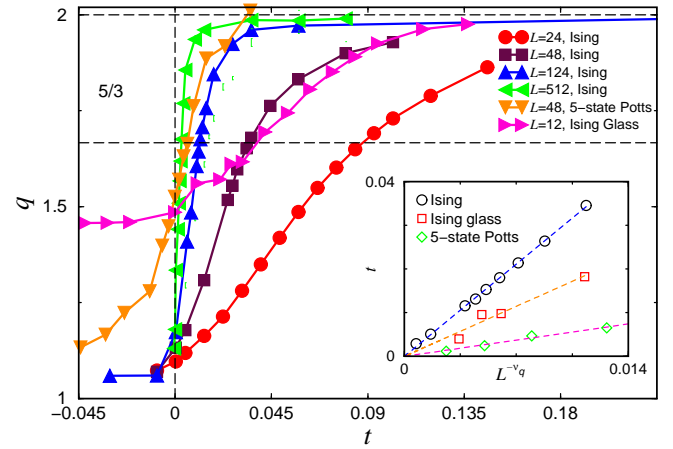


FIG. 4: Critical behaviour for all three models. The systems enter the Lévy regime when $q \geq q_c = 5/3$. When $q < 5/3$, the systems are in the Gaussian regime. For better view we have made some scale transformations: $t \rightarrow 5t$ for the 5-state Potts (with $N_{tw} = 80,000$) and $t \rightarrow t/5$ for the glass. Inset: Finite size scaling for all three models. The dashed lines are fitting lines. We show how the size-dependent critical temperature $T_{c,q}^L$ depends on the system size L . We mark $t = (T_{c,q}^L - T_{c,q})/T_{c,q}$ where $T_{c,q} = T_c$. We have made some scale transformations: $t \rightarrow 4t$ and $L^{-\nu q} \rightarrow 4L^{-\nu q}$ for the 5-state Potts model; $t \rightarrow t/20$ and $L^{-\nu q} \rightarrow L^{-\nu q}/10$ for the Ising glass model. We observe power-law dependence for all models.

Finally we evaluate the effect of the Cauchy noise which appears for all models. It is pronounced where D is far away from D_0 and its contribution is $pf_2(D) \sim \sigma_p/(D - D_0)^2$. We thus consider σ_p as a reliable quantity to measure the strength of the Cauchy noise. In the suitable range of N_{tw} , the σ_p of the Cauchy noise is invariant (see Fig. 2b and the Appendix D). We then study how it depends on the system size L for fixed q and suitable N_{tw} . As examples shown in Fig. 3, for both the 2-state Potts model from our general approach and the Ising model we find that it decays in power-law with the system size. This implies that for a macroscopic system the Cauchy contribution may go to zero and $P(D)$ is q -Gaussian in all ranges of D . We also study how the σ_p of the Cauchy noise depends on the parameter q for fixed L and N_{tw} . By comparing the results of two equivalent models mentioned above, we find that $P(D)$ from the former contains weaker Cauchy noise. Further, we also obtain better q -Gaussian fit to $P(D)$ of the Potts model which is constructed with fewer points (see Fig. 1).

Critical behaviour and multifractality

We now subtract the Cauchy noise and investigate the rest of $P(D)$, whose behaviour is related to macroscopic systems. In Fig. 4 we show for all three models how the value of q from a q -Gaussian fit depends on the reduced temperature $t = (T - T_c)/T_c$, where T_c is obtained from the conventional methods. For each finite system with the size L , we search for its corresponding critical temperature $T_{c,q}^L$. We employ this on different sizes of systems and all models. From the finite size scaling we have $T_{c,q}^L = aL^{-\nu q} + T_{c,q}$. We take the values of $T_{c,q}$ as those from conventional methods and find good power-

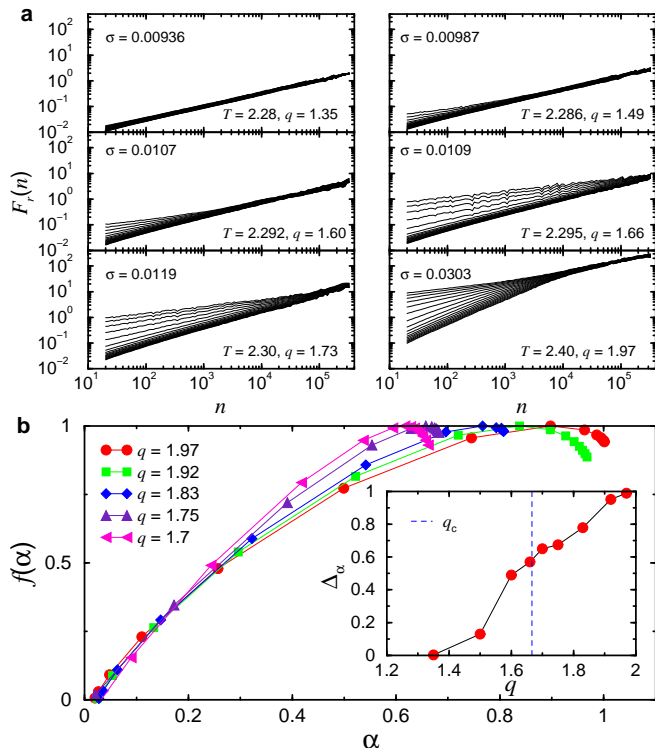


FIG. 5: Multifractal behaviour of the Ising model near the critical point. The system size is $L = 124$ and we have applied the MF DFA. The data have been shuffled before the calculation and the length of the order parameter ratio is 2 million. **a**, The fluctuation function $F_r(n)$ versus observing window n at different temperatures. Both the parameters q and σ are obtained from the q -Gaussian fit to the central part of $P(D)$. $F_r(n)$ are calculated in the ranges of $r \in [-4, 4]$ and $n \in (20, 327, 680)$. **b**, The singularity spectrum $f(\alpha)$ versus the singularity strength α for different values of q . The fitting range of n to obtain α and $f(\alpha)$ is $(20, 10,240)$. Inset: the range of the spectrum $\Delta_\alpha = \alpha_{\max} - \alpha_{\min}$ for different values of q .

law behaviours between $T_{c,q}^L - T_{c,q}$ and L (see inset of Fig. 4). The critical exponents ν_q for the Ising model, the Ising glass model and the 5-state Potts model are 1.16, 1.22 and 1.61, respectively. Thus the critical temperatures from our method is consistent with those from conventional considerations.

We next quantify the multifractality in signals using the multifractal detrended fluctuation analysis (MF DFA) [30, 37–39] (see the Appendix F), which is considered to be a reliable method to quantify the multifractal characteristic in a nonstationary series [5]. With this method we can calculate the r -th order fluctuation function $F_r(n) \sim n^{h(r)}$, where n is the size of the observing window. Varying $h(r)$ indicates the multifractality. We also calculate widely-used the singularity strength α and the singularity spectrum $f(\alpha)$. When $(\alpha, f(\alpha))$ spreads from one point to a variety of points in the X-Y plane, the multifractal behaviour appears.

In Fig. 5 with the Ising model as an example we show the multifractal behaviour of the shuffled series of the order parameter ratio where the time correlation is absent. Similar behaviour is also seen on other models (see the Appendix G). We find that the order parameter ratio is monofractal when

the corresponding q is far below $q_c = 5/3$. When we approach $T_{c,q}^L$ from the ordered phase, the slope of $F_r(n)$ gradually shifts from small scales of n for certain values of r . Yet at large scales all fluctuation functions still maintain the identical slope. At $q = q_c$ the multifractality appears at all scales we observe. Nevertheless, the range of n where the multifractality presents shrinks when continuing increasing the value of q . We further show the singularity spectrum $f(\alpha)$ v.s. α . We find that the spreading range of the spectrum $\Delta_\alpha = \alpha_{\max} - \alpha_{\min}$ is small for small $q < 5/3$, indicating a Gaussian-like monofractal behaviour. However when q approaches $5/3$, Δ_α rapidly increases and then slowly expands with increasing q .

The multifractal behaviour shown above should not be system specific since we have considered the shuffled series. To further verify this, we generate some q -Gaussian distributed artificial signals and set the same parameters for the artificial signals and the testing model (see the Appendix H). We find that the results are almost identical for the artificial signals and the model. Thus such multifractal behaviour is determined by the two parameters q and σ of the q -Gaussian distribution. To observe the multifractality, it requires $q \geq 5/3$. When $q > 5/3$, the range where the multifractality presents is controlled by σ . For fixed value of q , the larger size of system, the smaller value of σ (see the Appendix H). Correspondingly the larger system presents multifractal behaviour in broader range of n .

Conclusion

With tunable examples we have shown that physical systems near the phase transition present much more complex self-similar behaviour represented by the multifractality of the ratio of two order parameters measured at different spatial scales. At all temperatures around the critical point the distribution of the ratio follows a non-extensive q -Gaussian distribution plus a possible Cauchy background which decays in power-law with the system size and may disappear for a macroscopic system. The q -Gaussian distribution enters the Lévy regime at the critical point, and triggers the multifractality at all scales we observe. We have proposed a general approach which relates only to the broken symmetry yielding zero and non-zero order parameters in different phases as well as the self-similar characteristics of systems near the transition. Thus it should be applicable to other physical systems. The multifractality appears for the order parameter m obtained within suitable range of (time) scales where certain short-range properties of the specific system are lost and m shows good spatial self-similarity. In this situation the long-range correlation in the order parameter prevails and the ratio of order parameters follows a non-extensive q -Gaussian distribution. Our results suggest that the Tsallis q -statistics may play an important role in phase transitions.

This work is supported by the National Natural Science Foundation of China (Grant no. 11275184), Anhui Provincial Natural Science Foundation (Grant no. 1208085MA03), and the Fundamental Research Funds for the Central Universities of China (Grants no. WK2030040012 and 2340000034).

- [1] Plischke, M. & Bergersen, B. *Equilibrium Statistical Physics, 3rd Edition* (World Scientific, New Jersey, 2006).
- [2] Huang, K. *Statistical Mechanics, 2nd Edition* (John Wiley & Sons, New York, 1987).
- [3] Binney, J.J., Dowrick, N.J., Fisher, A.J. & Newman, M.E.J. *The Theory of Critical Phenomena: An Introduction to the Renormalization Group* (Oxford Univ. Press, New York, 1992).
- [4] Fisher, M.E. Renormalization group theory: Its basis and formulation in statistical physics. *Rev. Mod. Phys.* **70**, 653-681 (1998).
- [5] Kwapien, J. & Drozd, S. Physical approach to complex systems. *Phys. Rep.* **515**, 115-226 (2012).
- [6] Amitrano, C., Coniglio, A., Meakin, P. & Zanetti, M. Multi-scaling in diffusion-limited aggregation. *Phys. Rev. B* **44**, 4974-4977 (1991).
- [7] Jensen, M.H., Kadanoff, L.P., Libchaber, A., Procaccia, I. & Stavans, J. Global universality at the onset of chaos: Results of a forced Rayleigh-Bnard experiment. *Phys. Rev. Lett.* **55**, 2798-2801 (1985).
- [8] Muzy, J.F., Bacry, E. & Arneodo, A. Wavelets and multifractal formalism for singular signals: Application to turbulence data. *Phys. Rev. Lett.* **67**, 3515-3518 (1991).
- [9] Ivanov, P.Ch., *et al.* Multifractality in human heartbeat dynamics. *Nature* **399**, 461-465 (1999).
- [10] Ashkenazy, Y., Baker, D.R., Gildor, H. & Havlin, S. Nonlinearity and multifractality of climate change in the past 420,000 years. *Geophys. Res. Lett.* **30**, 2146-2149 (2003).
- [11] Bene, J. & Szeplafalusy, P. Multifractal properties in the one-dimensional random-field Ising model. *Phys. Rev. A* **37**, 1703-1707 (1988).
- [12] Castellani, C. & Peliti, L. Multifractal wavefunction at the localisation threshold. *J. Phys. A: Math. Gen.* **19**, L429-L432 (1986).
- [13] Mirlin, A.D., Fyodorov, Y.V., Mildenerger, A. & Evers, F. Exact relations between multifractal exponents at the Anderson transition. *Phys. Rev. Lett.* **97**, 046803 (2006).
- [14] Rodriguez, A., Vasquez, L.J. & Romer, R.A. Multifractal analysis with the probability density function at the three-dimensional Anderson transition. *Phys. Rev. Lett.* **102**, 106406 (2009).
- [15] Rodriguez, A., Vasquez, L.J., Slevin, K. & Romer, R.A. Critical parameters from a generalized multifractal analysis at the Anderson transition. *Phys. Rev. Lett.* **105**, 046403 (2010).
- [16] Tsallis, C. Possible generalization of Boltzmann-Gibbs statistics. *J. Stat. Phys.* **52**, 479-487 (1988).
- [17] Tsallis, C., Levy, S.V.F., Souza, A.M.C. & Maynard, R. Statistical-mechanical foundation of the ubiquity of Lévy distributions in nature. *Phys. Rev. Lett.* **75**, 3589-3593 (1995).
- [18] Baranger, M. Why Tsallis statistics? *Physica A* **305**, 27-31 (2002).
- [19] Hanel, R. & Thurner, S. When do generalized entropies apply? How phase space volume determines entropy. *Europhys. Lett.* **96**, 50003 (2011).
- [20] Tsallis, C. Nonextensive statistics: Theoretical, experimental and computational evidences and connections. *Brazilian Journal of Physics* **29**, 1-35 (1999).
- [21] Umarov, S., Tsallis, C. & Steinberg, S. On a q -central limit theorem consistent with nonextensive statistical mechanics. *Milan J. Math.* **76**, 307-328 (2008).
- [22] Douglas, P., Bergamini, S. & Renzoni, F. Tunable Tsallis distributions in dissipative optical lattices. *Phys. Rev. Lett.* **96**, 110601 (2006).
- [23] Liu, B. & Goree, J. Superdiffusion and non-Gaussian statistics in a driven-dissipative 2D dusty plasma. *Phys. Rev. Lett.* **100**, 055003 (2008).
- [24] Burlaga, L.F. & Ness, N.F. Compressible "turbulence" observed in the heliosheath by Voyager 2. *ApJ* **703**, 311-324 (2009).
- [25] Pickup, R.M., Cywinski, R., Pappas, C., Farago, B. & Fouquet, P. Generalized spin-glass relaxation. *Phys. Rev. Lett.* **102**, 097202 (2009).
- [26] Sotolongo-Grau, O., Rodriguez-Perez, D., Antoranz, J.C. & Sotolongo-Costa, O. Tissue radiation response with maximum Tsallis entropy. *Phys. Rev. Lett.* **105**, 158105 (2010).
- [27] Borland, L. Option pricing formulas based on a non-Gaussian stock price model. *Phys. Rev. Lett.* **89**, 098701 (2002).
- [28] Nakao, H. Multi-scaling properties of truncated Levy flights. *Phys. Lett. A* **266**, 282-289 (2000).
- [29] Drozd, S., Kwapien, J., Oswiecimka, P. & Rak, R. Quantitative features of multifractal subtleties in time series. *Europhys. Lett.* **88**, 60003 (2009).
- [30] Kantelhardt, J.W., *et al.* Multifractal detrended fluctuation analysis of nonstationary time series. *Physica A* **316**, 87-114 (2002).
- [31] Wolff, U. Collective Monte Carlo updating for spin systems. *Phys. Rev. Lett.* **62**, 361-364 (1989).
- [32] Bhatt, R.N. & Young, A.P. Numerical studies of Ising spin glasses in two, three, and four dimensions. *Phys. Rev. B* **37**, 5606-5614 (1988).
- [33] Chen, Z. & Yu, C.C. Comparison of Ising spin glass noise to flux and inductance noise in SQUIDs. *Phys. Rev. Lett.* **104**, 247204 (2010).
- [34] Landau, D.P. & Binder, K. *A Guide to Monte Carlo Simulations in Statistical Physics, 2nd Edition* (Cambridge University Press, Cambridge, UK, 2005).
- [35] Wu, F.Y. The Potts model. *Rev. Mod. Phys.* **54**, 235-268 (1982).
- [36] Wu, F.Y. Potts model and graph theory. *J. Stat. Phys.* **52**, 99-112 (1988).
- [37] Peng, C.-K., *et al.* Mosaic organization of DNA nucleotides. *Phys. Rev. E* **49**, 1685-1689 (1994).
- [38] Chen, Z., Ivanov, P.Ch., Hu, K. & Stanley, H.E. Effect of non-stationarities on detrended fluctuation analysis. *Phys. Rev. E* **65**, 041107 (2002).
- [39] Chen, Z., *et al.* Effect of nonlinear filters on detrended fluctuation analysis. *Phys. Rev. E* **71**, 011104 (2005).

Appendix

A. Self-similarity in distributions of the order parameter

When a system is in the vicinity of the critical point, many physical quantities of it display self-similar (scaling) properties. The distribution of the order parameter also shares this characteristic. In Fig. S1 we show an example for the 2-dimensional 5-state Potts model with the size $L = 96$. We construct the associated block spin system with size $L' = 96/4 = 24$ utilizing the standard coarse-graining procedure. For a d -dimensional spin system with L^d lattices, we can transform it into a block spin system with $(L/b)^d$ block spins. Each of block spins contains b^d spins. A coarse-graining operation is reached when we substitute each of block spins by

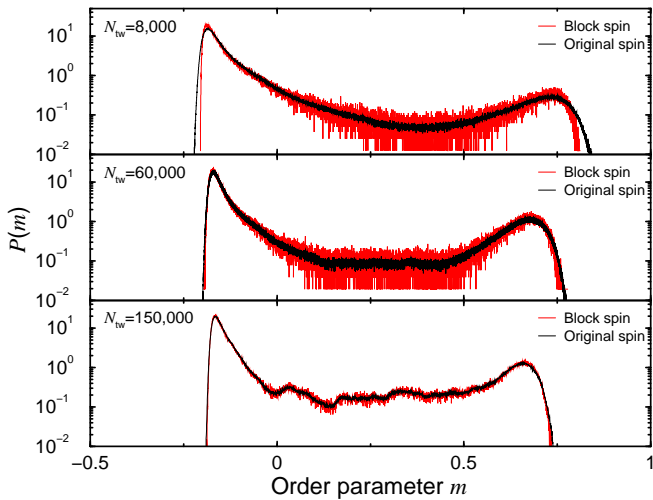


FIG. S1: Self-similarity of distributions of the order parameter for the 5-state Potts model. The system size is $L = 96$ and the temperature is $T = 0.8515$. For the distribution of the block (coarse-grained) spin system (with $L' = 96/4 = 24$) we have done the following scale transformation: $x \rightarrow x/1.215$, $y \rightarrow y \times 1.215$. With larger thermal averaging interval N_{tw} we obtain better similarity between the distribution of the original spin system and that of the block spin system.

a single spin with the value determined by the majority rule. For example, for the Ising model the block spin is +1 if there are more spins up than down, and *vice versa*. In particular, when the amount of spins up and spins down is equal, we assign the block spin +1 or -1 randomly. In this way we have constructed the Ising system at the scale “ b ”. The block spin system for the Potts model can be constructed similarly.

Nevertheless, for the Potts model we do not see good scaling when the thermal averaging interval N_{tw} for the order parameter m is too small (see Fig. S1). In this situation m contains certain short-range information specifically related to the Potts model. It is well-known that the critical properties of a physical system do not depend on the short-range details, but on the characteristics of long-range fluctuations. Such short-range information is not self-similar and may diminish with larger N_{tw} where the time correlation in the order parameter becomes weaker. (For example, see the Appendix E.) For sufficiently large value of N_{tw} , the distribution of the order parameter for the original system $h_1(x)$ and that for the block spin system $h_b(x)$ become similar, i.e., $h_1(x) = h_b(cx)/c$. Interestingly, when such scaling relation is effective, the distribution of the order parameter ratio $P(D)$ becomes symmetric and follows a q -Gaussian distribution, as we show in the paper.

B. Cauchy noise in distributions of the order parameter ratio

In Fig. S2 we present the Cauchy distributed fat tails in distributions of the order parameter ratio $P(D)$. For the Ising model we observe very good fit to the tails of $P(D)$ down to $10^{-4} - 10^{-5}$, while the length of the order parameter ratio is

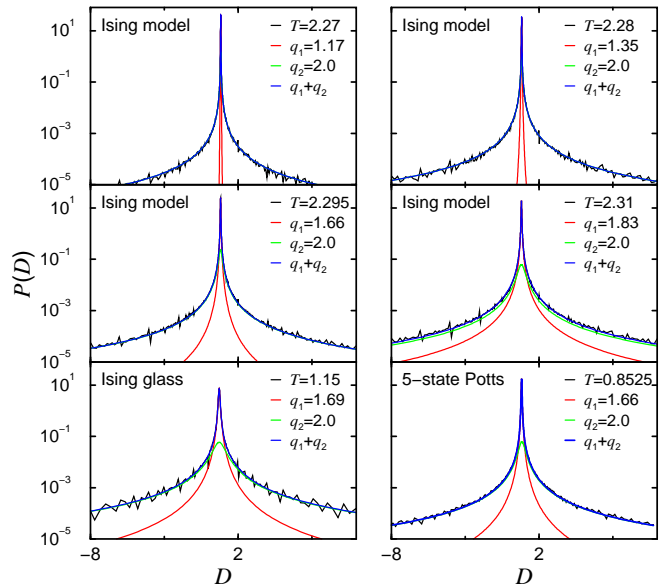


FIG. S2: Cauchy distributed fat tails in distributions of the order parameter ratio. We show such tails at different temperatures for all three models. The data are the same as those we show in Fig. 1 of the paper.

8-16 million. We also note that at high temperatures with q close to 2, the Cauchy background may be still pronounced. In an example shown in Fig. S2 for the system at $T = 2.31$ and with the size $L = 124$, we find that a single q -Gaussian fit works well for the central part, however it still underestimates $P(D)$ at positions of D far away from the peak D_0 .

The above behaviour has also been found in the Ising glass model and the Potts model. For the former at each temperature we have 150 samples each with 2 million points after the equilibrium. For the latter at each temperature the length of the order parameter ratio is 5.8 million. As examples in Fig. S2 we show such behaviour at the critical point $T_{c,q}^L$ which we have defined in the paper. For both models good fits to the tails of $P(D)$ down to 10^{-4} are observed.

C. Origin of the Cauchy noise

By reversing our procedure we can deduce the origin of the Cauchy distributed fat tails. To see this, we define a quantity $r(D) = \min[f_{\text{cauchyfit}}(D)/P(D), 1]$, where $f_{\text{cauchyfit}}(D)$ is our Cauchy fit and $P(D)$ is the distribution of the model from the Monte Carlo simulation. At each Monte Carlo step t with the order parameter ratio $D(t) = m(1, t)/m(b, t)$, we take $r(D)$ as the probability of this data point belonging to the Cauchy noise. We did this at each t and thus could obtain the corresponding $m(1, t)$ and $m(b, t)$ which belong to the Cauchy noise. Such considerations can be done in all ranges of D or in partial range of D , e.g., we can choose the range of D which is outside the cross points of the central part and the Cauchy part of $P(D)$. As shown in the orange and brown dashed lines of Fig. S3 we find that the distribution of $m(1, t)$ or $m(b, t)$ which is associated with the Cauchy part of $P(D)$ outside the

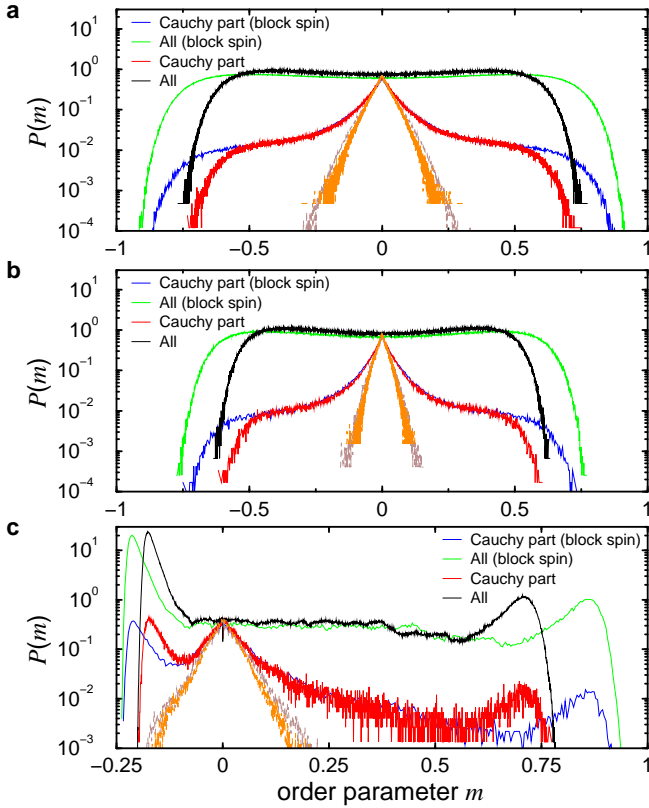


FIG. S3: Origin of the Cauchy noise as seen in the distribution $P(m)$ of the order parameter m . **a**, For the 2-dimensional Ising model at $T = 2.295$ with the size $L = 124$. **b**, For the 2-dimensional Ising model at $T = 2.275$ with the size $L = 512$. **c**, For the 5-state Potts model at $T = 0.851$ with the size $L = 48$, while the thermal averaging interval N_{tw} is 80,000. The values of q for the distributions of the corresponding order parameter ratio are 1.66, 1.66 and 1.45, respectively. The orange and brown dashed lines are contributed by the original and block spins associated with the Cauchy part of $P(D)$ outside the cross points with the central part of $P(D)$.

cross points with the central part of $P(D)$ achieves a local maximum and is symmetric about zero, then decays with approximately exponential tails for large values of m , indicating a disorder-like behaviour. Further, the tails decay faster for the system with larger size. This implies that the fat tails in $P(D)$ may go to zero when the system size $L \rightarrow \infty$. Such behaviour is also true when the distribution $P(m)$ of the order parameter is asymmetric.

D. Asymmetric and symmetric $P(D)$ with different N_{tw}

For the n -state Potts model with $n \geq 2$ we find that the distribution of the order parameter ratio is not symmetric when the thermal averaging interval N_{tw} is small, as shown in Fig. 2a of the paper. Further, such behaviour diminishes with larger values of N_{tw} . To characterize this, we can calculate the skewness of $P(D)$ around the peak D_0 . (In practice, the width of the region we choose to calculate is around $11\sigma - 12\sigma$, where σ is the scale parameter of the testing q -Gaussian fit to

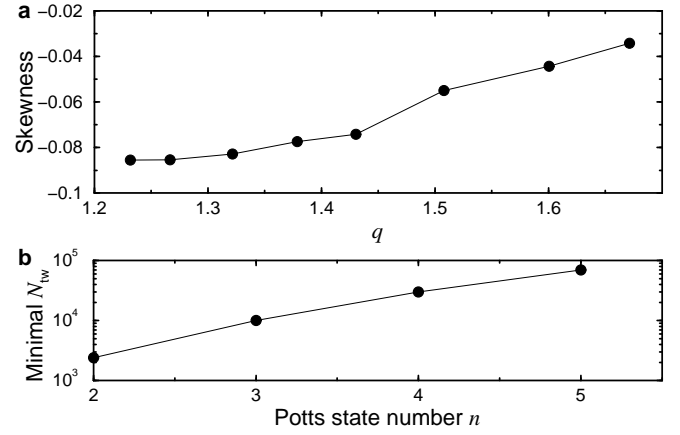


FIG. S4: Characteristics of the distributions of the order parameter ratio $P(D)$ for the Potts model. **a**, The skewness of the central part of $P(D)$ for the 5-state Potts model at temperatures with different values of q . We fix the system size $L = 36$ and the thermal averaging interval $N_{\text{tw}} = 16,000$. **b**, The dependence of the minimal N_{tw} at which one could obtain symmetric $P(D)$ on the Potts state number n at temperatures with fixed $q = 1.5$. We fix the system size $L = 48$. The skewness of the corresponding $P(D)$ is within $(-0.01, 0.01)$.

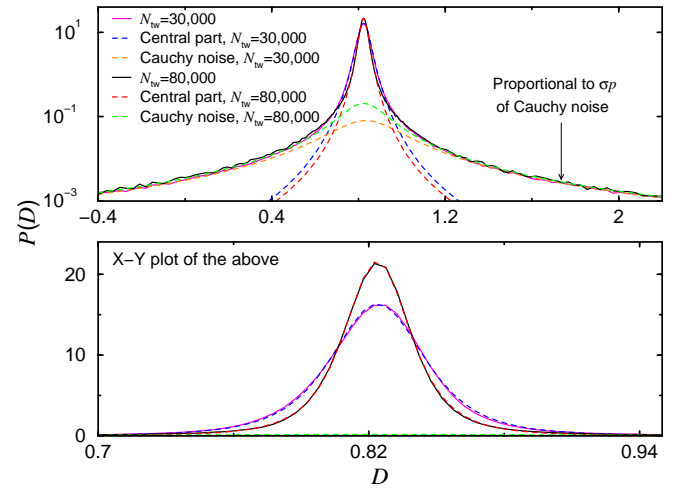


FIG. S5: Strength of the Cauchy noise for the 5-state Potts model. We fix the temperature $T = 0.8515$ ($q \sim 1.55$) and the size $L = 36$. For different values of N_{tw} within the suitable range, the strength represented by the σp of the noise keeps constant.

$P(D)$.) As shown in Fig. S4a, such asymmetry seems larger at lower temperature with smaller value of the parameter q . Further, it is also stronger for the Potts system with more possible spin states. This is manifested in Fig. S4b, where we fix the q -Gaussian fit parameter $q = 1.5$. We find that $N_{\text{tw}}^{\text{min}}$ — the minimal value of the thermal averaging interval N_{tw} to obtain symmetric $P(D)$ — increases with increasing value of the state number n . Specifically, we note that $N_{\text{tw}}^{\text{min}}$ is consistent with the results of the Ising model which is related to the 2-state case of the Potts model. Since for $n \leq 4$ the system has a second order phase transition, such behaviour is not related to the order of the transition.

For sufficiently large thermal averaging interval N_{tw} , $P(D)$

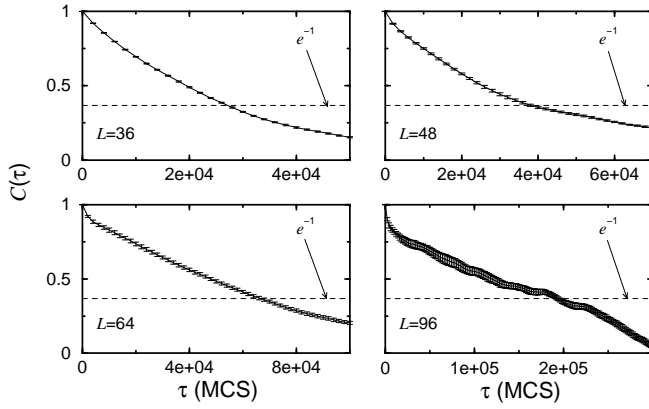


FIG. S6: Average time correlation in the order parameter m of the 5-state Potts model. We fix the temperature $T = 0.8515$ and vary the size of systems. The time delay τ_0 corresponding to $C(\tau) = 1/e$ is the characteristic time scale of interest.

becomes symmetric, and it would keep symmetric when continuing increasing the value of N_{tw} , as shown in Fig. 2b of the paper. Further, the value of the parameter q in a q -Gaussian fit to $P(D)$ also keeps almost invariant in a broad range of N_{tw} . Here we show some examples in Fig. S5. In this suitable range the strength of the Cauchy noise, marked by the σp of the noise, also keeps constant.

E. Time correlation in the order parameter time series

The order parameters which we obtain through Monte Carlo simulations may be correlated in time. Such correlation may be stronger when the system is in the vicinity of the critical point. As an example, here we investigate the 5-state Potts model near the phase transition. We fix the temperature $T = 0.8515$ and vary the size of systems. To obtain the time correlation function $C(\tau)$, for different sizes of systems we fix the thermal averaging interval $N_{\text{tw}} = 2,000$. The order parameter $m_{i,\alpha}$ of the Potts model depends on the spin value α and the spin index i . We also fix α and for each original spin i we calculate the time correlation $C_i(\tau)$. We show the average $C(\tau)$ of all original spins in Fig. S6. When the time decay τ is small $C(\tau)$ decays exponentially, i.e., $C(\tau) \sim \exp[-\tau/\tau_0]$ where τ_0 is the characteristic time scale. Comparing with the results we show in Fig 2b, we find that the distribution of the order parameter ratio $P(D)$ becomes symmetric when the thermal averaging interval N_{tw} is comparable or larger than the characteristic time scale of the order parameter m .

F. Multifractal detrended fluctuation analysis (MFDFA)

The multifractal detrended fluctuation analysis (MFDFA) is an efficient and reliable method available to quantify the multifractality in a non-stationary series. For a series $\{x_i\}$ with the length N , its procedure is the following:

(1) Calculate the profile

$$Y(j) = \sum_{i=1}^j [x_i - \langle x \rangle], j = 1, \dots, N,$$

where $\langle \dots \rangle$ is the mean of $\{x_i\}$.

(2) Divide $Y(j)$ into $N_n \equiv \text{int}(N/n)$ non-overlapping parts of length n . The maximal value of n should be smaller than $N/4$ to avoid statistically unreliable results. We perform this step from both the beginning and the end of the signal. Thus we totally obtain $2N_n$ parts.

(3) For each part with index ν we calculate the local trend $y_\nu^\ell(i)$ in this part by a least-square fit of the series with a polynomial function, where ℓ is the order of the polynomial function. We then subtract this local trend and determine the variance:

$$F^2(\nu, n) \equiv \frac{1}{n} \sum_{i=1}^n \{Y[(\nu-1)n+i] - y_\nu^\ell(i)\}^2,$$

for $\nu = 1, \dots, N_n$ and

$$F^2(\nu, n) \equiv \frac{1}{n} \sum_{i=1}^n \{Y[N - (\nu - N_n)n + i] - y_\nu^\ell(i)\}^2,$$

for $\nu = N_n + 1, \dots, 2N_n$.

(4) Average over all parts we obtain the r -th order fluctuation function:

$$F_r(n) \equiv \left\{ \frac{1}{2N_n} \sum_{\nu=1}^{2N_n} [F^2(\nu, n)]^{r/2} \right\}^{1/r}.$$

For $r = 0$ we choose

$$F_0(n) \equiv \exp \left\{ \frac{1}{4N_n} \sum_{\nu=1}^{2N_n} \ln [F^2(\nu, n)] \right\}.$$

(5) Determine the scaling of the fluctuation function: $F_r(n) \sim n^{h(r)}$. If $h(r)$ is a constant, the signal is monofractal; otherwise it is multifractal.

The singularity spectrum can be further calculated from: $f(\alpha) = r[\alpha - h(r)] + 1$, where the singularity strength $\alpha = h(r) + rh'(r)$. If the signal is monofractal, we find that $\alpha = h(r) = \text{const}$ and $f(\alpha) = 1$.

G. Multifractal behaviour of the 5-state Potts model

As another example here we investigate the multifractal behaviour of the 5-state Potts model in the vicinity of the critical point. We set the thermal averaging interval $N_{\text{tw}} = 80,000$ at all temperatures. After obtaining the series of the order parameter ratio, we first shuffle the data and then apply the MFDFA. The results of the fluctuation function $F_r(n)$ versus the observing window n are shown in Fig. S7. We find that, below the critical point (in the ordered phase) the system is monofractal since the slope of $F_r(n)$ is identical for different values of r . When approaching the critical point from

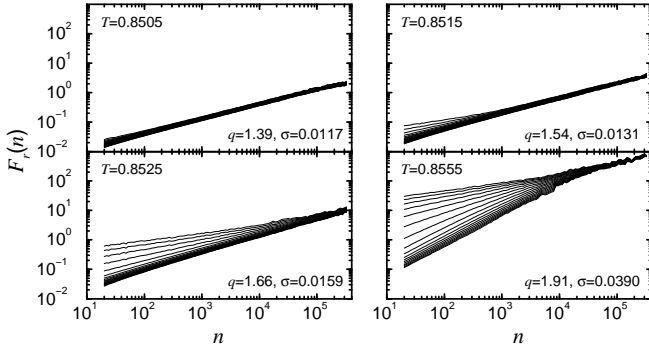


FIG. S7: Multifractal behaviour of the 5-state Potts model near the critical point. The system size is $L = 48$ and we have applied the MF DFA. The data have been shuffled before the calculation and the length of the order parameter ratio is 2 million. We set the thermal averaging interval $N_{tw} = 80,000$ at all temperatures. We show the fluctuation function $F_r(n)$ versus observing window n at different temperatures. Both the parameters q and σ are obtained from the q -Gaussian fit to the central part of $P(D)$.

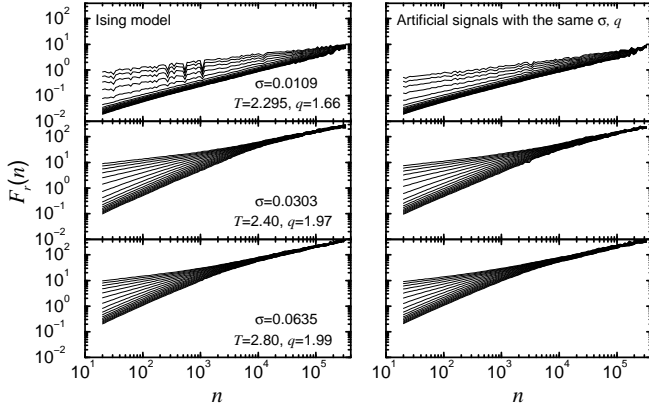


FIG. S8: Multifractal behaviour of the Ising model compared to that of q -Gaussian distributed artificial signals. The system size of the Ising model is $L = 124$. We set the same parameters σ and q for the artificial signals and the model. The data length is 1.6 million.

the ordered phase, the slope of $F_r(n)$ starts to shift at small scales, indicating a multifractal behaviour within these scales. Such region is broader when the system is closer to the critical point. At the critical point we observe multifractal behaviour at all scales we measure. When continuing increasing the temperature, the system is in the disordered phase. The value of the parameter q from the q -Gaussian fit is increasing while

the region where the multifractal behaviour presents shrinks. Such behaviour is similar to that of the Ising model. Nevertheless, for the Potts model we find that the scale parameter σ of the q -Gaussian fit is increasing with increasing temperature and fixed N_{tw} , while it is not sensitive to the temperature for the Ising model if the measured q is far below 2.

H. Characteristics of the multifractal behaviour

Here we investigate the characteristics of the multifractal behaviour we show in the paper. To do this, we generate some q -Gaussian distributed artificial signals and we set the same parameters for the artificial signals and for the testing model — the Ising model. For the model we have first shuffled the data thus eliminated the dynamics in signals. As shown in Fig. S8 we find that the results are almost identical for the artificial signals and the model when the parameters q and σ are the same. This verifies that the multifractal behaviour we present in the paper is not a system specific behaviour but should be applicable to other physical systems.

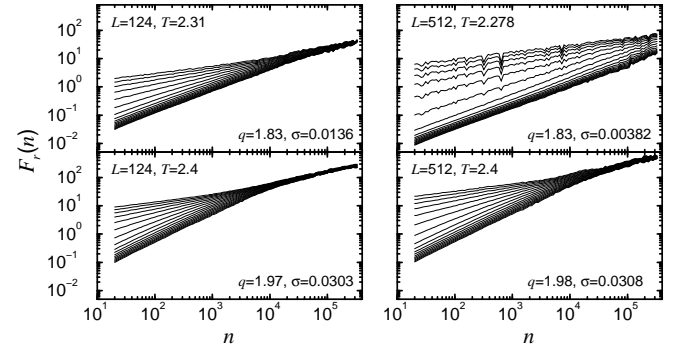


FIG. S9: System size dependence of the multifractal behaviour of the Ising model. The data length is 1.6 million.

We then investigate how the multifractal behaviour depends on the size of a specific system. Such dependence should be manifested from the values of two parameters q and σ . To see this, we investigate the Ising model with different sizes $L = 124$ and $L = 512$. We first shuffle the data and eliminate the dynamics in signals. We then apply the MF DFA and find that with the same parameter q , the difference in the observed multifractal behaviour is owing to different values of the scale parameter σ (see Fig. S9). When q is fixed, the larger system with smaller value of σ shows multifractal behaviour in broader region than the smaller system shows.